Conflict free trajectory optimisation for complex departure procedures

Santi Vilardaga
CTAE-ASCAMM
Cerdanyola del Vallès, Barcelona (Spain)
Email: santi.vilardaga@ctae.org

Xavier Prats
Technical University of Catalonia
Castelldefels, Barcelona (Spain)
Email: xavier.prats@upc.edu

***Abstract*—4D trajectory optimisation has showed good potential to reduce environmental impact in aviation, increase capacity and improve the efficiency of the operations. The research described in this paper proposes a dynamic optimiser for complex (and realistic) lateral and vertical trajectories, defined by a set of waypoints that define a flight plan. Different routes can be optimised independently, producing a vertical, lateral and speed profile that burns the minimum fuel. Additionally, may one conflict arise between two independent trajectories, each aircraft will recompute its optimal trajectory with separation assurance constraints defined as a cylindrical protection zone. Examples are given for standard instrumental departures at Barcelona and Reus airports. Different results are shown for strategies that allow both lateral and vertical deviations, or vertical deviations only. In a highly automated air traffic system the framework described in this paper enhances the situational awareness of the airspace user by providing information of the ownship energy state in accordance to the separation with the surrounding traffic.**

I. Introduction

The improvement of air transport efficiency (in terms of economic and environmental impact) is one of the major drivers for research and development in the SESAR and NextGen programmes. New technologies and procedures for future air traffic management (ATM) and on-board systems and operations are being investigated and proposed. Initiatives such as Continuous Climb Departures (CCD), Continuous Cruise Climb (CCC), and Continuous Descent Approaches (CDA) propose good fuel reduction in specific phases of the flight. However, such operations usually come with a negative impact in air traffic capacity, given the vast typologies of aircraft and hence diversity in vertical and speed profiles [1].

To this end, algorithms and methods that improve efficiency and capacity in the airspace whilst maintaining, if not improving, safety are being proposed. For example, several research has been done in the integration of CDAs in dense TMAs [2], [3]. The Oceanic Tailored Arrivals program, currently in place in San Francisco airport [4], is another relevant example. These arrivals are supported by the Efficient Descent Advisor (EDA) developed by NASA-AMES, which is able to compute conflict-free optimal descent trajectories and satisfy a given arrival fix metering [5]. Being the EDA a ground based system, it lacks from accurate aircraft performance data, since airspace users in general, do not publish what they consider is subject to confidentiality.

One requirement for efficient flow of air traffic is accurate knowledge of aircraft positions and adequate prediction of future aircraft movements. Without accurate information, maintaining safe separation between aircraft requires much more conservative, and therefore less efficient, methods [6], [7]. Moreover, a large scale implementation of these optimised trajectories (i.e. not only for a small set of aircraft but for all those in a dense and complex TMA) remains an issue that will obviously require more levels of automation.

Nowadays, the literature on optimal arrival trajectories is very extended when compared to that regarding optimised aircraft departures. Still, some studies are investigating this aspect, for example [8], [9], [10]. However, the de-confliction with other traffic is a big technical challenge to address. Usually, separation assurance on the TMA (for arriving and departing trajectories) is ensured at a strategic level, via complex lateral profiles and imposing altitude and velocity constraints at the standard procedures (e.g. level off departing traffic below an incoming traffic's corridor). Additionally, the operating air traffic ATCo may enforce the separation at a tactical level if required. Such operations prevent the aircraft to fly optimised trajectories (i.e. CDA and CCD), increasing fuel and pollutant emissions and producing a larger noise impact in the vicinities of the airport. Besides, new enhanced operations allow for a window of opportunity to optimise (or deconflict) where there was previously a traffic corridor.

Via an own developed trajectory optimisation framework and following previous research presented in [11] this paper aims at the optimisation of conflict free trajectories in a dense traffic area, including separation constraints with surrounding traffic. Using an A320 dynamic model, we generate a very fast initial guess of the trajectory, that is immediately afterwards optimised using a continuous multiphase optimal control problem formulation, taking into account spatial and temporal constraints. We are using our algorithms to show results on how two conflictive departures can be optimised whilst maintaining safety levels with self separation strategies.

This paper is organised as follows. Section II lays out the dynamic model of the aircraft, the problem formulation and the trajectory modelling in multiple phases. Section III enhances the optimisation framework to include separation assurance constraints. Section IV describes the scenarios and results that we have obtained. Finally, section V presents our conclusions.

II. Optimisation framework

Trajectory modelling and optimisation has been a subject widely researched in the last decades. Analytically, this optimisation problem can be formally written as a continuous optimal control problem and extensive research on its resolution can be found in the literature. However, realistic trajectories are hardly impossible to solve analytically and a wide variety of numerical solutions have arisen. One of the most relevant ones involves the direct transcription of the problem, leading to a non-linear programming (NLP) problem with a finite set of decision variables [12]. This approach sets-up the basic theoretical background for the research proposed in this paper.

A. Equations of motion

For this research, we are using a point-mass representation of the aircraft, where forces apply at its centre of gravity. For the initial assessment proposed in this paper, a winds calm situation, in a flat non-rotating earth has been assumed. Thus, and assuming a constant mass of the aircraft, the equations of motion are written as follows [8]:

$$\begin{array}{rcccl} \frac{\mathrm{d}v}{\mathrm{d}t} & = & \dot{v} & = & \frac{1}{m}(T - D - mg\sin\gamma) \\ \frac{\mathrm{d}\gamma}{\mathrm{d}t} & = & \dot{\gamma} & = & \frac{g}{v}(n_z\cos\phi - \cos\gamma) \\ \frac{\mathrm{d}\chi}{\mathrm{d}t} & = & \dot{\chi} & = & \frac{g}{v}\frac{\sin\phi}{\cos\gamma}n_z \\ \frac{\mathrm{d}n}{\mathrm{d}t} & = & \dot{n} & = & v\cos\gamma\cos\chi \\ \frac{\mathrm{d}e}{\mathrm{d}t} & = & \dot{e} & = & v\cos\gamma\sin\chi \\ \frac{\mathrm{d}h}{\mathrm{d}t} & = & \dot{h} & = & v\sin\gamma \\ \frac{\mathrm{d}s}{\mathrm{d}t} & = & \dot{s} & = & v\cos\gamma \end{array} \tag{1}$$

where n and e represent the spatial location of the aircraft in north and east coordinates respectively, h is the geometric altitude, v is the true airspeed, γ the aerodynamic flight path angle, χ the heading and ϕ the bank angle. Also, s represents the along track distance, calculated to take into account some constraints that depend on it. The load factor (n_z) is defined as the relation between the aerodynamic lift force and the aircraft weight.

Regarding the atmosphere, the International Standard Atmosphere [13] model is considered, which defines the density ρ, pressure p and temperature τ magnitude as functions of the altitude. The following normalised magnitudes are also used in this paper:

$$\delta = \frac{p}{p_0}; \quad \theta = \frac{\tau}{\tau_0}; \quad \sigma = \frac{\rho}{\rho_0}; \tag{2}$$

where p_0, τ_0 and ρ_0 are, respectively the standard pressure, temperature and density values at sea level.

B. Drag and thrust models

The aerodynamic drag is given as a function of the drag coefficient (C_D), dynamic pressure (q), and wing reference area (S) as:

$$D = C_D q S. \tag{3}$$

The total drag coefficient C_D is expressed as a function of the lift coefficient C_L and the Mach number M. This relationship considers air compressibility effects, which cannot be neglected for nominal cruising speeds of typical commercial aircraft (between M.78 and M.82 approximately). In this paper, a polynomial fitting similar to the model proposed in [14], giving a very accurate approximation of the drag coefficient:

$$C_D = C_{D0} + K_i\left(C_L - C_{L0}\right)^2 + C_{Dsb}\left(\beta\right) \tag{4}$$

where C_{Dsb} accounts for the speedbrakes contribution and $\beta \in [0,1]$ is the speedbrake lever position.

Coefficients C_{D0}, K_i and C_{L0} depend on the flaps/slats setting and M. For each aircraft configuration these coefficients are obtained after a fitting function process with aircraft aerodynamic data obtained from manufacturer's performance databases:

$$\begin{aligned} C_{D0} &= C_{D0_{min}} + \Delta C_{D0} M \\ K_i &= K_{i_{min}} + \Delta K_{i_1} M + \Delta K_{i_2} M^2 \\ C_{L0} &= C_{L0_{min}} + \Delta C_{L0_1} M + \Delta C_{L0_2} M^2. \end{aligned} \tag{5}$$

Regarding the engine model, Airbus A320 throttle positions (π) directly command the revolutions of the engine fan ($N1$). The throttle also takes values in the interval $[0,1]$ and is modelled as:

$$\pi = \frac{N1 - N1_{idle}}{N1_{max} - N1_{idle}}. \tag{6}$$

The maximum revolutions of the engine fan $N1_{max}$ and the residual revolutions, when the throttle is set to zero ($N1_{idle}$) are also modelled with a 3^{rd} degree polynomial approximation as:

$$N1_k = \sum_{i=0}^{3}\sum_{j=0}^{3} c_{ij}^k \theta^i M^j \quad k \in \{max, idle\}. \tag{7}$$

Following the same methodology, engine thrust (T) and fuel flow (FF) are also modelled by a third order polynomial as a function of the reduced revolutions of the engine fan ($N1/\sqrt{\theta}$) and the Mach number:

$$\begin{aligned} T &= n_e \delta \sum_{i=0}^{3}\sum_{j=0}^{3} c_{ij}^T \left(\frac{N1}{\sqrt{\theta}}\right)^i M^j \\ FF &= n_e \delta \sqrt{\theta} \sum_{i=0}^{3}\sum_{j=0}^{3} c_{ij}^{FF} \left(\frac{N1}{\sqrt{\theta}}\right)^i M^j \end{aligned} \tag{8}$$

being n_e the number of engines of the airplane.

C. Problem formulation

Optimal control problems are usually non-linear and generally do not have analytic solutions so it is required to employ numerical methods to solve them [12], [15]. The most popular approach is to convert the infinite-dimensional original problem into a finite-dimensional NLP problem in the time interval $[t_0, t_f]$. To do so, a collocation strategy is performed, being Euler, Trapezoidal or Pseudospectral among the most used [16]. The value of t_f is a decision variable itself and will be fixed by the optimisation algorithm.

Let $\boldsymbol{x}(t) \in \mathbb{R}^{n_x}$ be the state vector describing the trajectory of the aircraft over the time t, $\boldsymbol{u}(t) \in \mathbb{R}^{n_u}$ the control vector that leads to a specific trajectory and $\boldsymbol{p} \in \mathbb{R}^{n_p}$ a set of control parameters not dependent on t. The goal is to find the best trajectory that minimises the following optimisation objective:

$$\boldsymbol{J}(t) = \int_{t_0}^{t_f} FF(\boldsymbol{x}, \boldsymbol{u}, \boldsymbol{p}, t)\, \mathrm{d}t. \tag{9}$$

Using the equations of motion and aerodynamic forces described above, we have formulated an optimal control problem, the solution to which minimises the fuel consumption as defined in (9). The state and control vectors are defined as follows:

$$\begin{aligned} \boldsymbol{x} &= [\ v\ \ \gamma\ \ \chi\ \ n\ \ e\ \ h\ ] \\ \boldsymbol{u} &= [\ n_z\ \ \phi\ \ \pi\ ]. \end{aligned} \tag{10}$$

Since the operating manuals of the aircraft give minimum and maximum operating speeds in calibrated airspeed (CAS), we add an extra constraint equation to relate this speed with the true airspeed that appears in (1):

$$v_{CAS} = \sqrt{\frac{2p_0}{\mu\rho_0}\left[\left(\delta\left(\left(\frac{\mu v^2}{2R\tau}+1\right)^{\frac{1}{\mu}}-1\right)+1\right)^{\mu}-1\right]} \tag{11}$$

where $\mu = \frac{\gamma_a - 1}{\gamma_a}$, being γ_a the specific heat ratio of the air and R the perfect gas constant.

Table II-C depicts the constraints considered in the optimisation problem. Many of these are operational constraints, either to stay within the flight envelope or comply with ATM constraints such as ground obstacle avoidance (PDG). Additionally, bounding constraints on n_z and ϕ where defined following usual civil aviation standards. More information on optimal control formulation techniques used in this research can be found in [17], [18].

Finally, some collocation and link equations ensure that the different state nodes (collocation points) within a phase are correctly linked to the previous in compliance with the dynamic models, and that the phases relate to the time continuum they represent as explained in the following subsection.

D. Multiphase modelling

An aircraft departing trajectory comprehends different flight phases with specific performance values to each phase. In it, there is a first phase where the aircraft will be at maximum take-off thrust climbing up without the possibility of turning or making changes in the aerodynamic configuration. In many studies, this phase is not contemplated given the low degrees of freedom that pose these operational constraints. After that, the following phases are defined by aerodynamic changes (flaps/slats retraction) and thrust cutback. Since flap retraction will change aircraft performance, each phase has different aerodynamic drag coefficients among other particularities. In our framework, these aerodynamic configuration changes are executed at predefined speed steps.

TABLE I
CONSTRAINTS IN THE OPTIMAL CONTROL PROBLEM

Constraint	Definition
Operating airspeeds	$V_{MCA} \leq v_{CAS}(t) \leq VMO$
No deceleration allowed	$\dot{v}(t) \geq 0$
No descent allowed	$\dot{h}(t) \geq 0$
Procedure Design Gradient (PDG)	$h(t) \geq 3.3\% s$
Load factor	$0.85 \leq n_z(t) \leq 1.15$
Bank angle	$-25 \leq \phi(t) \leq 25$

Besides, the departing aircraft follows a route specified by a set of vertical and lateral constraints described in the standard procedure (SID). This can be simplified to a list of waypoints at a specific latitude and longitude. Additionally, these may also have altitude and speed constraints and eventually a requested time of arrival (RTA) as given by an ATCo at a tactical level.

In the previous paragraphs we have specified two disconnected types of phases: those related to aerodynamic configuration of the aircraft (e.g. changes in flaps, gear, etc.) and those related to operational restrictions (changes in direction, altitudes, etc.). Both define intrinsic phases that cannot be correlated. In other words, the order of which operational events occur is independent to the order of which lateral events occur. For example, a waypoint indicating a turn on the procedure could be before or after the moment the aircraft transitions from an aerodynamic configuration to the following one. Even for the same aircraft type, depending on the weather conditions and the mass of the aircraft the order of these events will differ. Hence, this apparently simple problem becomes hard to solve with the sole use of phases. We explain in the following paragraphs our solution to this issue, based on the use of switching functions.

To take into consideration the changes in aerodynamic configurations, we use continuous and twice differentiable switching functions. This method has the negative impact that it adds complexity (non-linearities) to the model (greater computational times and possible convergence difficulties), and the minor side effect of having a transition effect around the switching value. Both issues are directly related, since the less steep is the function at the switching point (and thus smoother for the NLP Solver) the bigger is the transition effect, and vice versa. Hence, a trade-off must be sought [18].

This strategy allows the use of phases to define the lateral (and vertical) route. With this, we are able to compute a full

trajectory from a set of initial conditions to a set of final conditions, including one or more RTA in waypoints along the route using a constrained multi-phase optimal control problem.

III. Conflict free optimisation

Having different trajectories being modelled in a scenario, the main challenge remains in modelling the separation assurance constraint. Current ATC procedures specify lateral and vertical separation independently given the big difference in dynamics between the horizontal and vertical plains: either 3Nm or 5Nm in horizontal and 1000ft or 2000ft in vertical space, depending on technical and environment related aspects [19]. Thus, we consider a *conflict* if there is a risk of an aircraft entering this protection volume unless deviation manoeuvres are deployed. This could lead to a loss of separation and eventually to a near mid-air collision or ultimately a fatal encounter.

In a futuristic scenario, we could envisage that the aircraft themselves are responsible for keeping separation amongst each other, thus delegating ATC responsibilities to the pilot. Current developments on that aspect depend on the use of airborne separation assurance systems (ASAS) [20]. The experiments within this paper assume such paradigm is in place.

Besides, collaboration between aircraft is an important issue to address. A very utopic scenario would assume a fully collaborative situation where centralised trajectory optimisation is possible due to downlink of aircraft performance data and intends. Nowadays, airlines are very wary on providing such information to other airspace users. Hence, another (less collaborative) solution is to use a flight plan or flight intends to predict other aircraft trajectories. This solution relies on ADS-B/C data or the implementation of collaborative methodologies such as AIDL [21] or SWIM [22]. In such case, a conflicted user can perform ownship optimisation separating from a prediction of other traffic future states. This paper explores a possible implementation and implications of this semi-collaborative scenario where an aircraft, instead of receiving performance data from other traffic, computes its own optimal deviation to avoid the conflict over a predicted intruder trajectory. This deconfliction aims at tactical traffic separation either because strategic deconfliction is inexistent, or it has failed due to big uncertainties at the time of deployment.

A. Separation assurance

NLP solvers demand each and every constraint to be continuous and twice differentiable, and it is obvious that a cylinder does not comply with this. To solve this issue one can describe the following disjunction:

$$g_h(t) \geq 0 \vee g_v(t) \geq 0 \tag{12}$$

being g_h and g_v the horizontal and vertical constraints respectively, which can be reformulated with continuous variables as described in [23] as follows:

$$\begin{aligned} \lambda_h(t) g_h(t) + \lambda_v(t) g_v(t) &\geq 0 \\ \lambda_h(t) + \lambda_v(t) &= 1 \\ \lambda_h(t), \lambda_v(t) &\geq 0 \end{aligned} \tag{13}$$

being λ_h and λ_v two continuous variables that, with the second and third constraints in (13), enforce the logical OR in this formulation.

Other strategies could bring better convergence to the algorithm with the cost of less accurate solutions. This would be the case for example of a sphere [24], an ellipsoid [25] or a superegg[1]. All these are geometrical forms that can be expressed by a single equation and, specifically to our problem, enforce separation by form of inequations. In contrast to the current cylindrical specification, the sphere is highly inaccurate in the term that treats lateral and vertical separation equally and ellipsoids are also very inaccurate at the extremes (i.e. the vertical separation is soon lost when going towards the edges). Supereggs on the other side are similar to ellipsoids but maintain the vertical separation longer. They can be represented by the following equation:

$$\left(\frac{n^2 + e^2}{{d_h}^2}\right)^2 + \left(\frac{h^2}{{d_v}^2}\right)^2 \geq 1 \tag{14}$$

where d_h and d_v are the required horizontal and vertical separation respectively, and n, e and h the state variables as defined in (1).

Even if it is out of the scope of this paper to thoroughly study each strategy, we have implemented both the cylindrical disjunction described in (13) and the supereggs inequation described in (14). The first because it represents exactly the current operations; and the second because it is still quite an accurate representation of the protection volume, but presents less non-linearities for the model, and thus performs very well on the optimisation engine.

The separation strategy described in this section is easily extrapolated to multiple conflicts.

B. Intruder trajectory modelling

As presented previously in this section, our problem requires an aircraft to recalculate an optimal trajectory that separates from other traffic. We have explained in section II how do we model the ownship. In III-A we have laid down some strategies for the aircraft to keep distance from a target object in space. The remaining challenge is how to model a moving target in our optimisation problem.

Our approach to this has been to represent the state of the moving target following polynomials that depend on time. Because a trajectory can be a very complex curve, we rely on polynomial fitting to model a predicted reference trajectory [26]. To this end, we assume that we have a high fidelity representation of the intruder's trajectory as a list of points in time and space. In our case, we are not actually relying on trajectory prediction strategies, but we are actually optimising

[1] http://en.wikipedia.org/wiki/Superegg

the route of the intruder first, and then passing the resulting trajectory over to the ownship. Then, this list of 4D points is modelled into curves represented by basis splines (B-splines) using the open source library *einspline*[2].

A Cubic B-spline is a continuous twice-differentiable function represented by piecewise polynomials of order three. As opposed to higher degree polynomials, these provide an accurate fitting and have been demonstrated to perform well with NLP optimisation [17] as they can be very smooth.

Effectively, this solution has proved very reliable, robust and with good performance in our simulations. Our approach is to create three splines that represent the intruder's north, east and altitude coordinates over time. At the optimisation process, the ownship will iteratively call these curves that represent the dynamic obstacle at each time of sampling (t).

Figure 1 depicts the flow of events of an aircraft (ownship), separating from an intruder in our framework.

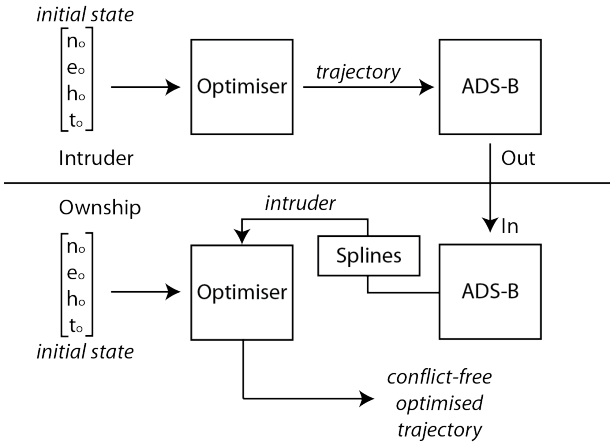

Fig. 1. Flow of events of aircraft separation on this paper

In the case where there is still a will for collaboration, both aircraft would compute own deviations and would agree (involving ATC) on the final manoeuvre, given a set of comparable variables, such as consumed fuel, the resulting time of arrival, etc.

C. Fixed lateral route

In current concept of operations, standard procedures are in place so conflicts are prevented at a strategic level. These remove lateral freedom to aircraft. To mimic this, we have implemented an option in the optimisation framework that fixes the lateral profile to the optimised trajectory. Thus, all deviations to avoid a conflict will be in altitude and speed profiles. The resulting trajectories are compared to show the impact of such restrictions in the results section.

To model the lateral fixed trajectory, we are again using splines. Since we have already demonstrated the benefits of them in the intruder trajectory, we are following a similar approach. In this case, we are generating the curves for the horizontal coordinates with respect to the along track distance s. Then, the n and e variables in the state vector will be constrained following these splines over s:

$$\begin{aligned} n(t) &= \Gamma_n(s(t)) \\ e(t) &= \Gamma_e(s(t)) \end{aligned} \tag{15}$$

where Γ_n and Γ_e are the splines modelling the lateral movement of the aircraft.

We understand that fixing the lateral profile to such precision is unrealistic. Specially because the freedom in the speed profile should result in different radius of turns for different velocities. Nevertheless, being aware of that, the nature of the results is still valid.

IV. Numerical example

The optimisation framework developed in this paper uses a combination of C++ and General Algebraic Modeling System (GAMS[3]) source code. GAMS is used for the facility it gives of implementing optimal control problems and the multiple NLP solver engines to which it seamlessly links. This characteristic allows for the different optimisation needs to be easily tested with different constraints and solvers without much effort. On top of that, a C++ wrapper has been developed to allow for a more flexible definition of scenarios, the generation of a guess and facilitate the interface with the splines library described in section III-A.

This design allows for dynamic definition of scenarios via waypoints and operational constraints as coming from a flight plan. For the purpose of this paper, we have prepared two scenarios following real life operations in two major airports in the Catalonia region. First scenario departs Barcelona airport (LEBL) on the west configuration through GRAUS3W SID. Second scenario departs Reus airport (LERS) to the east flying the BCN1S SID. At Barcelona, the west configuration is chosen by default, even in slight tail wind conditions (up to 10kts). In such case, Reus would have the east configuration.

Figure 2 shows the lateral route for both trajectories (red and blue respectively) as resulting from the optimiser, overlaid to the charts defined in the AIP[27], [28]. An Airbus A320 model has been considered for both departures and the lateral routes have been described as a list of waypoints as described in previous sections, assuming a flat non-rotating earth on a calm winds situation.

If figure 2, it is clear how BCN1S makes a big detour to strategically minimise potential conflicts with traffic departing from Barcelona. Indeed, if we describe a direct route to BCN VOR/DME after the initial climb (9NM from RES VOR/DME), the resulting trajectory is much more efficient than BCN1S (let us call this third route DIRECT). However, the strategic separation assurance strategy implemented in the AIP is lost. Hence, the appearance of conflicts is more likely to occur. We present a case where the separation between one aircraft flying DIRECT and another one flying GRAUS3W is less than the required protection zone (see case A in figure

[2]http://einspline.sourceforge.net/

[3]https://www.gams.com

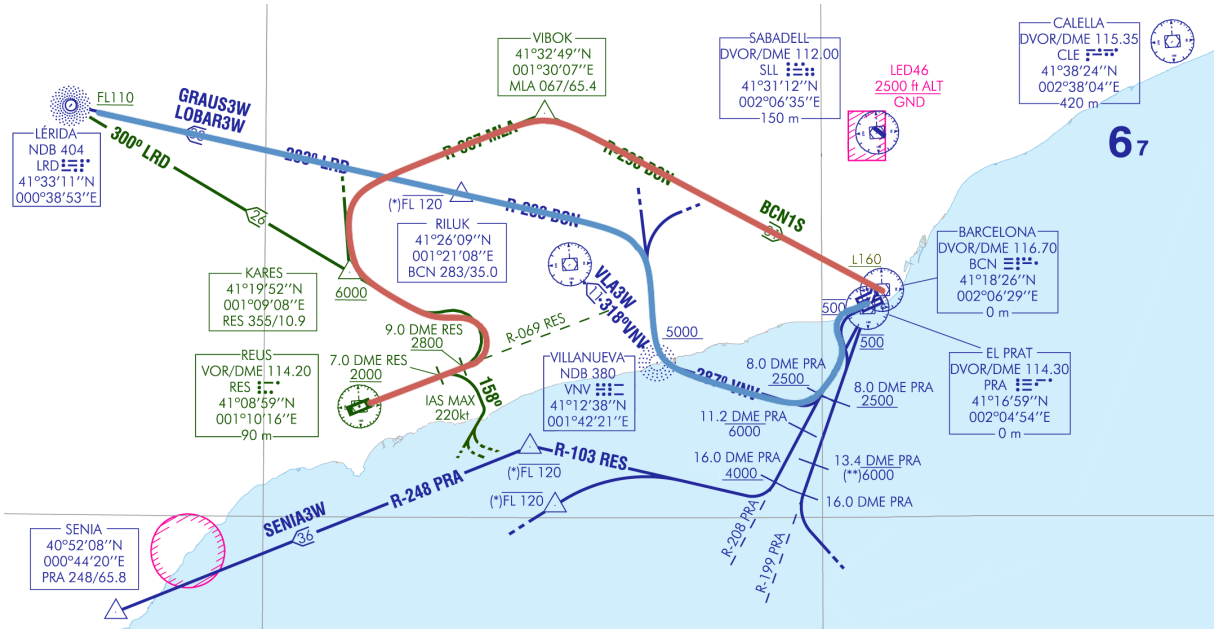

Fig. 2. Published standard instrumental departures for Barcelona (blue) and Reus (green) and optimised trajectories for Barcelona departure GRAUS3W (light blue) and Reus departure BCN1S (red)

3). Even so, in a futuristic scenario, where self-separation is in place, this new trajectory is worth studying.

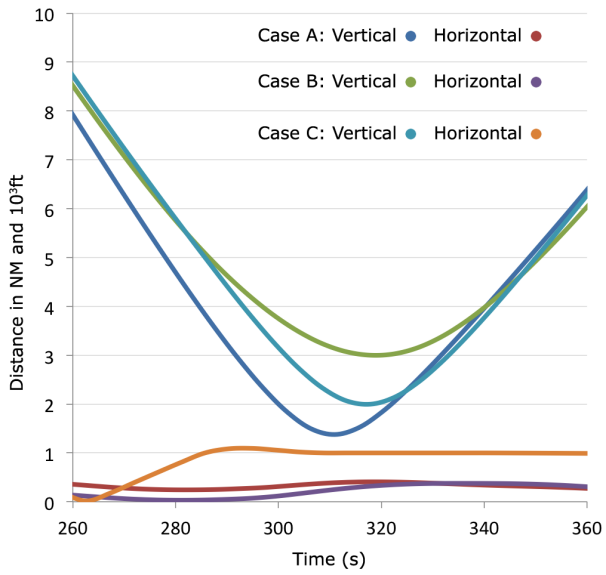

Fig. 3. Vertical and horizontal separation between the trajectories in cases A, B and C.

We then define a self-separation strategy with 3NM (case B) and 5NM (case C) as a horizontal constraint and 1000ft in the vertical domain. We deliver results on how much should this proposed trajectory deviate from the optimal in figure 4, 5 and 6, showing the lateral, vertical and speed profiles respectively that prevent the conflict. For the sake of a fair comparison we have added new waypoints to all trajectories to make sure the aircraft have enough time to reach cruise altitude (in the examples FL300), and such, a comparable energy setting. The separation between the aircraft is now preserved as depicted in figure 3.

We can see how, for case B, it is more efficient to deviate mostly on the horizontal domain, whereas case C combines lateral and vertical deviations.

Alternatively, cases D and E study the scenario where the aircraft in GRAUS1W is deviated instead (3NM and 5NM respectively). In these, we can see how the optimal relies almost only on the vertical domain. Of special interest, see in table IV how case E consumes less than case D, when it should be the other way around. We attribute this to a local optimal in case D due to either a bad guess or the disjunction in (13). Indeed, cases D and E have been also optimised using supereggs (cases F and G respectively) and this effect is removed. Also, with this strategy a better solution is found for both cases, mainly due to the shape of the superegg that allows for some minor incursion on the edges of the protection volume (see figure 7).

The horizontal deviations shown in 4 for some of the trajectories, may not be acceptable for current operations, given the lack of lateral freedom in the standard terminal procedures. This scenario is also studied in this paper as case H with the model described in section III-C. The results are less optimal, but still much better than the current BCN1S SID.

Table IV shows the different characteristics and results for the cases A to H in a summarised form.

Finally, such study can be also extended to include other passing traffic (i.e. more than one intruder trajectory in the problem). Besides, it could also include descending trajectories. In a scenario were many trajectories have to be checked

TABLE II
SUMMARY OF COSTS FOR THE DIFFERENT CASES

Scenario	Route	Separation	Time (s)	Dist (NM)	Fuel (Kg)	Time Diff (s)	Dist Diff (m)	Fuel Diff (Kg)
Ref	GRAUS3W	None	1279.48	227684.68	1534.80	-	-	-
Ref	BCN1S	None	1483.40	270583.45	1682.63	-	-	-
Case A	DIRECT	None	1142.71	203131.42	1440.61	-340.69	-67452.03	-242.02
Case B	DIRECT	Cylinder - 3NM / 1000ft	1139.71	203512.29	1442.52	-3.00	380.87	1.91
Case C	DIRECT	Cylinder - 5NM / 1000ft	1140.83	203376.35	1445.62	-1.88	244.93	5.01
Case D	GRAUS3W	Cylinder - 3NM / 1000ft	1280.96	227667.03	1539.74	1.48	-17.65	4.94
Case E	GRAUS3W	Cylinder - 5NM / 1000ft	1280.93	227634.93	1537.96	1.45	-49.75	3.16
Case F	GRAUS3W	Superegg - 3NM / 1000ft	1281.91	227671.89	1535.80	2.43	-12.79	1.00
Case G	GRAUS3W	Superegg - 5NM / 1000ft	1282.61	227634.03	1536.12	3.13	-50.65	1.32
Case H	DIRECT	Cylinder - 3NM / 1000ft	1107.16	203131.42	1451.15	-35.55	0.00	10.54

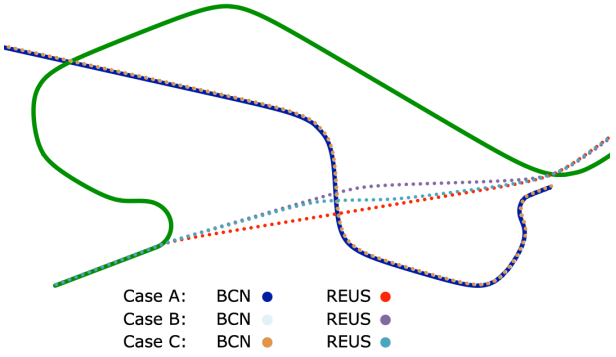

Fig. 4. Lateral profiles for the different optimised routes over the AIP charts for Reus and Barcelona

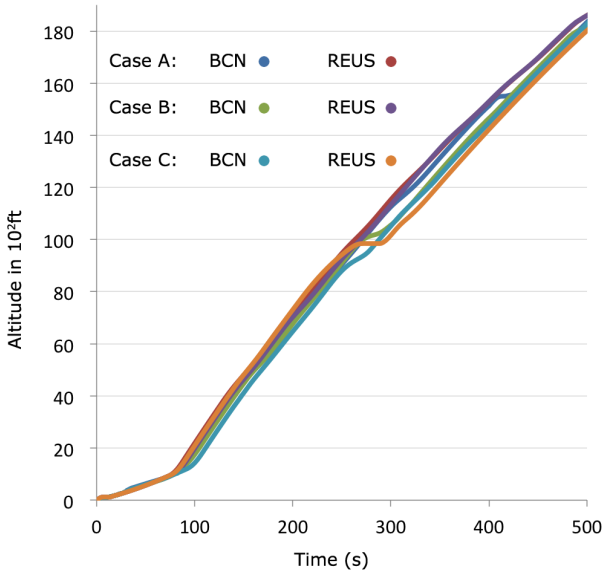

Fig. 5. Vertical profile for the different optimised routes

when designing a new standard procedure, the optimisation framework described in this paper provides good advise.

V. CONCLUSION AND FURTHER WORK

In this paper we have described a framework for optimising 4D trajectories in a lateral, vertical and speed profile per-

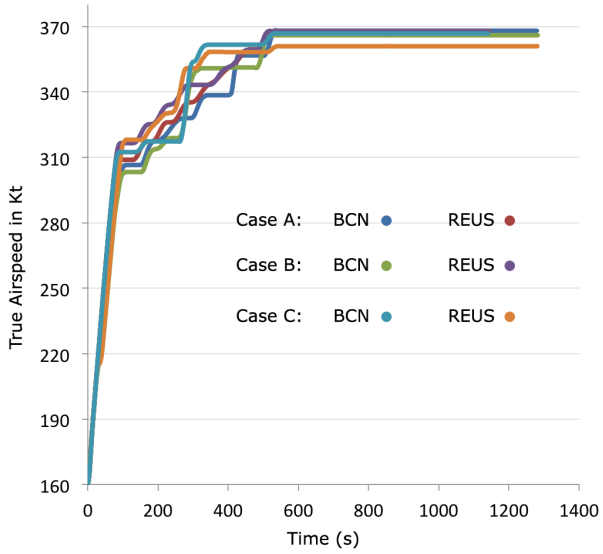

Fig. 6. Speed profile for the different optimised routes

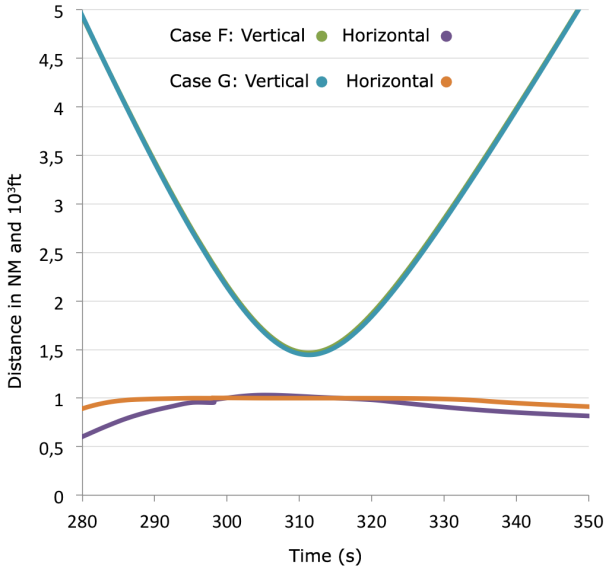

Fig. 7. Horizontal and vertical distances for cases F and G using supereggs

spective, while keeping separation to other traffic (assuming ASAS). We use direct collocation methods to convert the complex problem to a continuous multiphase optimal control problem that is solved with NLP techniques.

We consider a semi-collaborative scenario where trajectory predictions are shared between airspace users. This framework will be extended to accept different degrees of collaboration. First, a fully collaborative scenario in a futuristic automated environment where optimisation is done globally to all aircraft. Then, a complete un-collaborative scenario, where the only known data from the intruder is the current state vector. Given the fact that the trajectory estimation in this last case will be very inaccurate, techniques for target tracking and conformance monitoring will be introduced. Hence, recalculations will occur either when new information arrives, or when the tracker alerts of a deviation from the expected trajectory.

We have presented a not far from the reality scenario where our framework could be used as a decision support tool when designing a new procedure in an area with the confluence of many trajectories. Given the flexibility on the definition of scenarios in our tool, many other cases could be easily modelled. Besides, this could also be used with incoming vs outgoing traffic, very interesting nowadays that the new procedures (CDA, CCD, etc.) are more and more practiced and old traffic corridors become obsolete.

Finally, as explained in the results section we have encountered potential issues with local minima with the cylinder disjunction, whereas these are not seen when using supereggs. The impact of the different separation assurance techniques will have to be further investigated.

ACKNOWLEDGMENT

The authors would like to thank Airbus Industrie for the use of PEP (Performance Engineers Program) suite, which allowed us to undertake realistic aircraft performance simulations. Also, GTD for their support on the use and adaptation of the *einspline* library within GAMS.

REFERENCES

[1] C. M. Johnson, "Analysis of Top of Descent (TOD) Uncertainty," in *Digital Avionics Systems Conference (DASC), 2011 IEEE/AIAA 30th*. IEEE, 2011, pp. 1–10.

[2] A. Kuenz, V. Mollwitz, B. Korn, and F. Guidance, "Green Trajectories in High Traffic TMAs," *, 2007. DASC'07. IEEE/AIAA 26th*, 2007.

[3] N. T. Ho and J.-P. B. Clarke, "Methodology for Optimizing Parameters of Noise-Abatement Approach Procedures," *Journal of Aircraft*, vol. 44, no. 4, pp. 1168–1176, Jul. 2007.

[4] R. A. Coppenbarger, R. Lanier, D. Sweet, and S. Dorsky, "Design and Development of the En Route Descent Advisor (EDA) for Conflict-Free Arrival Metering," in *Metering, Proceedings of the AIAA Guidance, Navigation, and Control Conference*, 2004, pp. 1–19.

[5] R. A. Coppenbarger, R. Mead, and D. Sweet, "Field evaluation of the tailored arrivals concept for datalink-enabled continuous descent approach," in *AIAA Aviation Technology, Integration and Operations Conference (ATIO)*, vol. 46, no. 4, 2007.

[6] K. Roy, B. Levy, and C. Tomlin, "Target tracking and estimated time of arrival (ETA) prediction for arrival aircraft," *... of AIAA Guidance, Navigation, and Control ...*, no. August, pp. 1–22, 2006. [Online]. Available: http://arc.aiaa.org/doi/pdf/10.2514/6.2006-6324

[7] J. Tadema, E. Theunissen, R. Rademaker, and M. Uijt de Haag, "Evaluating the impact of sensor data uncertainty and maneuver uncertainty in a conflict probe," in *Digital Avionics Systems Conference (DASC), 2010 IEEE/AIAA 29th*, vol. 6, 2010.

[8] X. Prats, "Contributions to the optimisation of aircraft noise abatement procedures," Ph.D. dissertation, 2010.

[9] ERAT, "Final Report," ERAT Consortium, Sixth Framework Programme, E.C., Tech. Rep., 2012.

[10] S. J. Hebly and H. G. Visser, "Advanced noise abatement departure procedures: custom optimized departure profiles," *AIAA Guidance, Navigation and Control*, no. August, pp. 1–11, 2008.

[11] S. Vilardaga and X. Prats, "Effects in fuel consumption of assigning RTAs into 4D trajectory optimisation upon departures," in *3rd International Conference on Application and Theory of Automation in Command and Control Systems (ATACCS)*, no. 1, 2013.

[12] J. T. Betts, *Practical methods for optimal control and estimation using nonlinear programming*, 2nd ed., ser. Advances in design and control. Society for Industrial and Applied Mathematics, 2010, no. 19.

[13] ICAO, "Manual of the ICAO Standard Atmosphere: Extended to 80 Kilometres (262500 Feet)," International Civil Aviation Organization, Montreal, Canada, Tech. Rep., 1993.

[14] M. Kaiser, M. Schultz, and H. Fricke, "Enhanced jet performance model for high precision 4D flight path prediction," in *Proceedings of the 1st International Conference on Application and Theory of Automation in Command and Control Systems (ATACCS)*, 2011, pp. 33–40.

[15] I. M. Ross and F. Fahroo, "A Perspective on Methods for Trajectory Optimization," in *AIAA/AAS Astrodynamics Specialist Conference and Exhibit*, ser. Guidance, Navigation, and Control and Co-located Conferences. American Institute of Aeronautics and Astronautics, Aug. 2002.

[16] A. V. Rao, "A survey of numerical methods for optimal control," *Advances in the Astronautical Sciences*, 2009. [Online]. Available: http://vdol.mae.ufl.edu/ConferencePublications/trajectorySurveyAAS.pdf

[17] J. T. Betts and E. J. Cramer, "Application of Direct Transcription to Commercial Aircraft Trajectory Optimization," *Journal of Guidance, Control and Dynamics*, vol. 18, no. 1, pp. 151–159, 1995.

[18] S. Hartjes, H. Visser, and S. Hebly, "Optimisation of RNAV noise and emission abatement standard instrument departures," *Aeronautical Journal*, 2010.

[19] ICAO, "Procedures for Air Navigation Services. Air Traffic Management," 14th ed., International Civil Aviation Organisation, doc. 4444, Montreal (Canada), Tech. Rep., 2001.

[20] Eurocontrol, "Review of ASAS Applications studied in Europe," CARE/ASAS Action. CARE/ASAS Activity 4, Technical report, 2002.

[21] E. Gallo, J. Lopez-Leones, M. Vilaplana, F. Navarro, and A. Nuic, "Trajectory computation Infrastructure based on BADA Aircraft Performance Model," *2007 IEEE/AIAA 26th Digital Avionics Systems Conference*, 2007.

[22] SESAR, "Sistem Wide Information Management. ATM Information Reference Model," SESAR, Tech. Rep., 2012.

[23] A. U. Raghunathan, V. Gopal, D. Subramanian, L. T. Biegler, and T. Samad, "Dynamic optimization strategies for three-dimensional conflict resolution of multiple aircraft," *Journal of guidance, control, and dynamics*, vol. 27, no. 4, pp. 586–594, 2004.

[24] K. Mohan, M. Patterson, and A. V. Rao, "Optimal Trajectory and Control Generation for Landing of Multiple Aircraft in the Presence of Obstacles," in *Guidance, Navigation, and Control Conference*, no. August. Minneapolis, Minnesota: American Institute of Aeronautics and Astronautics, 2012, pp. 1–16.

[25] P. K. Menon, G. D. Sweriduk, and B. Sridhar, "Optimal Strategies for Free Flight Air Traffic Conflict Resolution," *Journal of Guidance, Control and Dynamics*, pp. 1–35, 1997.

[26] C. Gong and A. Sadovsky, "A Final Approach Trajectory Model for Current Operations," in *10th AIAA Aviation Technology, Integration, and Operations (ATIO) Conference*. Reston, Virigina: American Institute of Aeronautics and Astronautics, Sep. 2010.

[27] AENA, "Normalised Departure Chart. Standard Instrumental Procedure for Barcelona / El Prat. RWY25L / RWY20," Aeronautical Information Publication. AENA., Tech. Rep., 2012.

[28] ——, "Normalised Departure Chart. Standard Instrumental Procedure for Reus. RWY07," Aeronautical Information Publication. AENA., Tech. Rep., 2010.